# ORTHOGONAL WAVE CURRENT INTERACTION OVER A FIXED RIPPLED BED: PRELIMINARY RESULTS OF AN EXPERIMENTAL CAMPAIGN

Carla Faraci[1], Alessia Ruggeri[1],
Massimiliano Marino[2], Rosaria E. Musumeci[2] and Enrico Foti[2]

This paper reports some results obtained in the framework of the TA WINGS, funded by the EU through the Hydralab+ program. The project was aimed at investigating the hydrodynamic effects of an orthogonal wave onto a current in order to understand the nature of the velocity distribution along the water column over fixed ripples. Velocity profiles were acquired within the DHI shallow water tank by means of several Vectrinos in order to investigate the effects of wave-current interaction. A comparison between wave only case and wave plus current case showed that, when the current overlaps to waves, the recirculating cells formed near the bed are flatter than those formed in wave only. Moreover, the vorticity increases outside the boundary layer and decreases inside it when the current superposes to the wave.

*Keywords: orthogonal wave current interaction; fixed rippled bed; wave boundary layer; recirculating cells; vorticity*

## Introduction

The flow near the coast is usually influenced by the simultaneous presence of waves and currents. The interactions of waves and currents are complex hydrodynamic phenomena that can produce significant changes in mean velocity profile, in the structure of the boundary layer and in the sediment transport. A fundamental role in this process is given by bed roughness. Indeed, when the current is superimposed on the wave alone, the flow velocity at the bottom increases for small roughness and decreases for large roughness (Faraci et al. 2008). A rippled bed, in such circumstances, behaves like a large roughness, involving that wave boundary layer to become turbulent and the bed roughness to increase up to an order of magnitude in the presence of waves and currents (Fredsøe et al., 1999).

Some of the most relevant studies concerning the velocity behavior and the vorticity fields over a rippled bed in the presence of wave only are, for instance, Ranasoma and Sleath (1994), O'Donoghue et al. (2006), Scandurra et al. (2000), Earnshaw and Greated (1998). Fewer studies exist in literature focused on wave-current interaction and on vorticity study, e.g., Fredsøe et al. (1999), Faraci et al. (2008) and Faraci et al. (2018).

Ranasoma an Sleath (1994) carried out measurements of velocity over concrete ripples, for a steady current parallel to the ripple crests. O'Donoghue et al. (2006) through a large-scale experimental investigation in two oscillatory flow tunnels found that, in presence of ripples, the velocity generates an offshore directed transport of sediments.

Faraci et al. (2008) through the study of velocity profiles over a rippled bed, found that the existence of recirculating cells in the lower part of the water column generates modification of velocity profile and in particular a reversal of the velocity itself. Moreover, they observed that near bed velocity distribution for orthogonal wave and current interaction is double peaked and a key role is played by the vorticity dynamics (Faraci et al. 2018).

Earnshaw and Greated (1998) carried out an experimental campaign for the case of wave only on a fixed bed with polystyrene ripples, measuring within boundary layer with a Particle Image Velocimetry (PIV). The results showed that a vortex grew and is ejected in correspondence of the ripple crest at all flow conditions. The experimental conditions were used for validation of a discrete-vortex numerical model that foresaw both vortex strengths and trajectories.

A comparison between the wave only case and combined collinear flow case was carried out by Fredsøe et al. (1999); they observed that even when the current overlaps the wave, the behavior near the bed doesn't show great variations with respect to the wave only case.

From a numerical point of view, Faraci et al. (2008), by means of a $k$-$\omega$ turbulence closure numerical model, found that, for both wave only case and wave plus current case, vortices detach at phase 0-45° over the crest and the vorticity decreases in contemporary presence of wave and current. The different of the latter with Fredsøe is due to probably the shape of ripple profile being that the vorticity is greater over sharper bedforms (Horikawa and Mizutani 1992). In fact, the ripples used by Faraci have a less sharp crest than those of Fredsøe et al. (1999) study.

This work reports an experimental campaign carried out in the framework of the Transnational Access WINGS- Waves plus currents INteracting at a right anGle over rough bedS, funded by the EU

[1] Department of Engineering, University of Messina, 98166 Messina, Italy; cfaraci@unime.it
[2] Department of Civil Engineering and Architecture, University of Catania, 95123 Catania, Italy;

Commission through the Hydralab+ program. During this campaign tests of current only, wave only and waves plus current over three different bed were carried out.

In this paper, the study of mean flow field and vorticity over rippled bed are reported comparing between wave only case and wave plus current case in order to show what variations occur when the current superimposes the waves both inside the boundary layer and moving away from the bed.

**Experimental set up and Instrumentations**

The experimental campaign was carried out at the DHI (Danish Hydraulic Institute, Horsholm, DK). A shallow water tank (35m x 25m) allows conditions of current only, wave only and waves and currents to be reproduced simultaneously. Inside the tank, indeed, a system of three pumps that allowed a recirculating maximum flow rate of 1 $m^3/s$ and a wave maker array 18 m long were located. The wave maker array was composed by 36 panels, each one respectively 0.5 m wide and 1.2 m high, controlled by a software (Wave Synthesizer) through which the time duration of the tests and the wave height and period can be set up. Moreover, the software allows regular or random waves and angle of attack between wave and current ranging between 30° and 90° to be reproduced. For this campaign only 90° angle was used since the focus was on orthogonal wave and current interaction.

Figure 1 shows a sketch of the shallow water basin with the reference system chosen in such a way that the current direction is coincident with the *x*-axis, the wave direction with *y*-axis and *z*-axis is positive upwards.

To provide energy absorption and control of the reflection, a passive parabolic wave absorber and a C-shaped mixed gravel beach sloped by 1/5.6 were used contemporaneously.

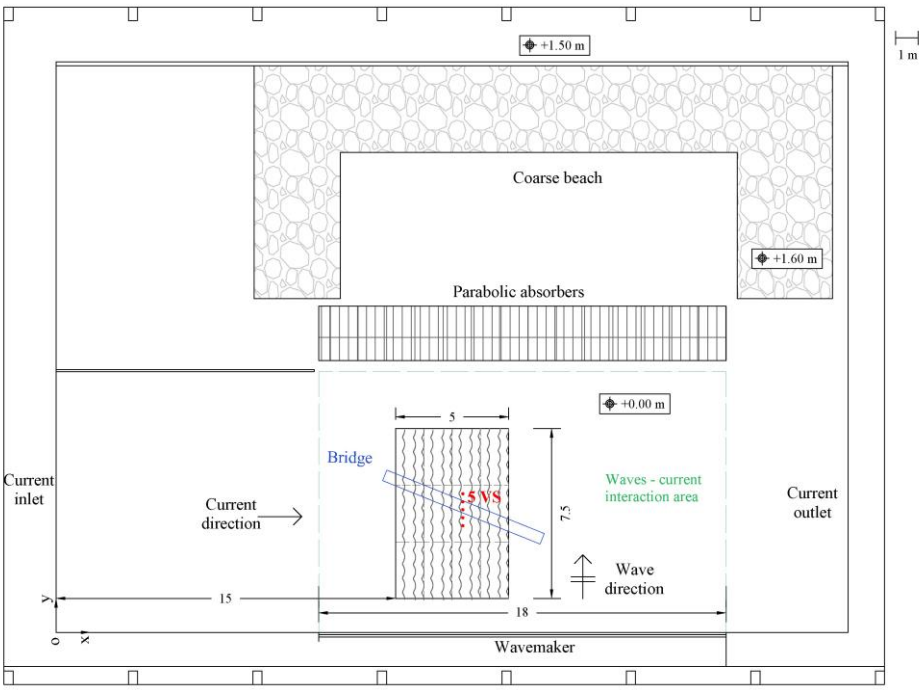


**Figure 1. Sketch of the Shallow water tank of the Danish Hydraulic Institute.**

The wave-current interaction area, sketched in green in Figure 1 was chosen after preliminary tests (Ruggeri et al. 2020) that identified the most suitable area where the instrumentation could be placed, verifying that the local coordinates influenced the flow velocity at a minor extent.

During the experimental campaign, tests were carried out varying water depths ($d$=0.6 m and $d$=0.4 m), wave periods ($T$=2 s and $T$=1 s) and wave heights ($H$=0.12 m $H$=0.08m and $H$=0.05 m).

A rippled bed area of 5.0 m x 7.5 m was created with 12 wood panels (1.25 m x 2.5 m) on which several corrugated plastic panels properly modeled were fixed. These panels were modelled in order to obtain the required ripple characteristics (ripple wavelength $\lambda$=125 mm and ripple height $\eta$=18.5 mm). The panels were spread with homogeneous layer of glue, the ripple crests were properly sharpened through a wooden model and they were sprinkled with sand ($d_{50}$=0.9 mm) to obtain a proper roughness.

Moreover, some scale effects must be taken into account, as for as fixed rippled bed was considered, considering that wave and current characteristics were changed during the experimental

campaign. However, the dimensions of fixed ripple profile (length $\lambda$ and height $\eta$) were carefully chosen based on the results of previous experimental campaigns (Faraci et al. 2012, 2019 and Petrotta et al 2018), in order to be the most statistically frequent.

A rendering of the tank was realized with ARCHICAD software and a sketch of the laboratory is shown in Figure 2. In details, in central part of the tank the bridge which support part of instrumentations, to the left the two absorption systems and to the right the wave maker are located. Moreover, two different work stations for data acquisition, one near the absorption systems and other near the wave maker were placed.

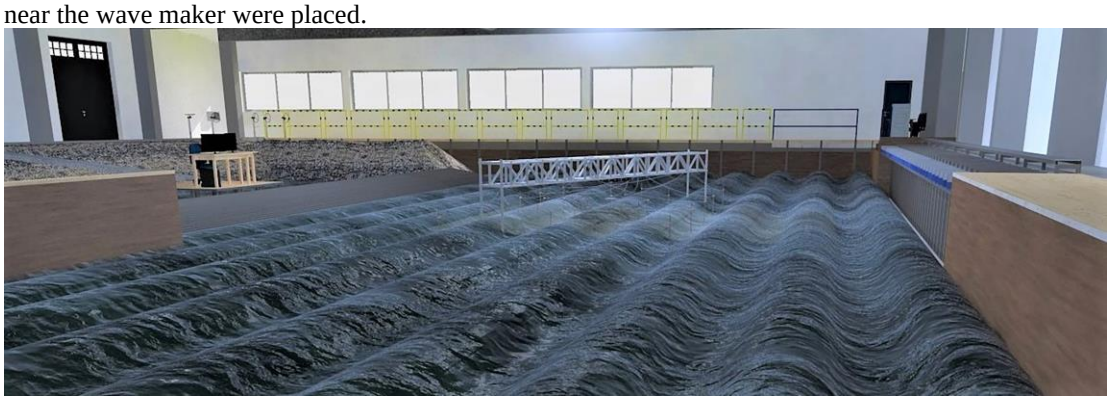

**Figure 2. Rendering of the tank trough use of software ARCHICAD**

24 resistive wave gauges were located in the waves-current interaction area to recover the free surface and 5 of them were disposed according to Faraci et al. (2015) for the study of wave reflection. A maximum reflection was found at $x$=18 m, equal to 20% in the WO case while, when the current superposes the wave, this effect is reduced to 5% (Ruggeri et al. 2020).

To acquire the velocity profiles, five Vectrino Single-Point (high-resolution Acoustic Doppler Velocimeters by Nortek As.) were used. Four of them were down-looking and one side-looking. The Vectrino were held equidistant each other through a trolley and positioned along wave direction over the ripple profile (see Figure 3).

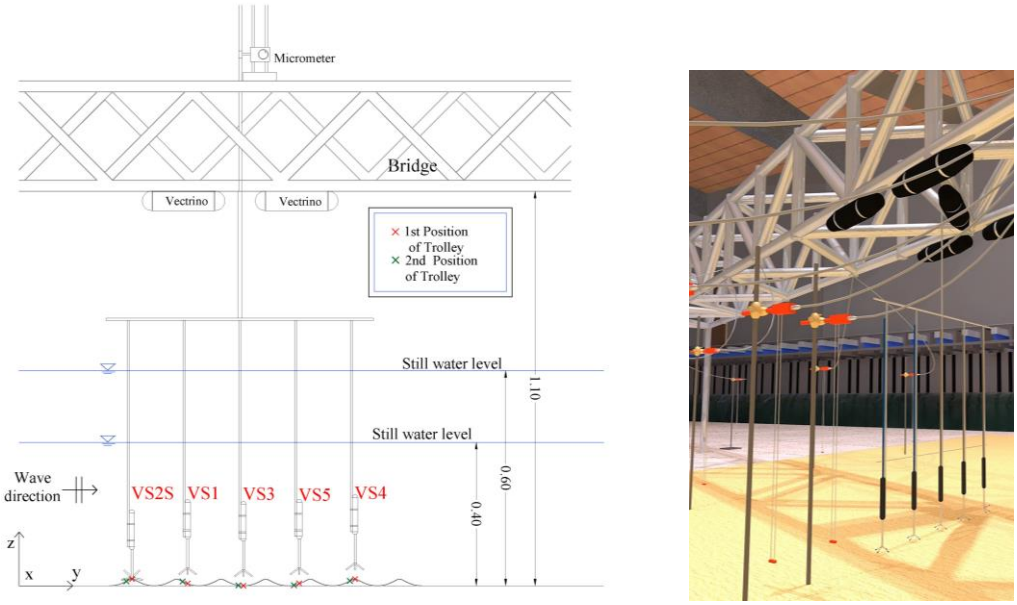


**Figure 3. Bridge with instrumentation. (a) Sketch of the trolley with both measuring points of Vectrino over ripples; (b) Rendering of Instrumentation (wave gauges in red and Vectrino in black).**

Two position of trolley were considered by sliding the trolley by 1/8 of ripple length. More precisely, in Figure 3a red crosses on the ripple profile correspond to measuring point for the first position of trolley, green crosses to the second one. By doing so, 9 measurement points are obtained on a single ripple profile, thus being able to obtain more accurate information on the flow field.

The sampling volume of the Vectrino is located 50 mm far from the transducer and its dimensions can be modified via the acquisition software in relation to the desired quality of the signal; the sampling rate is up to 200 Hz.

The reliability of the measured velocities is related to two parameters namely Correlation (COR) and Signal to Noise Ratio (SNR), (see e.g.van der Zanden et al., 2017; Yoon and Cox, 2010). Two acceptance thresholds were adopted: COR ≥ 90 and SNR ≥ 30 near the sweet spot, i.e., from 50 to 65 mm below the transceiver, SNR ≥ 20 elsewhere. Non-reliable data were replaced by linear interpolation. Finally, data were despiked by means of the Goring and Nikora (2002) method.

### Analysis of the experimental results

During the experimental campaign tests of current only (CO), wave only (WO) and waves and currents (WC) were carried out. In particular 18 tests (2 CO, 8 WO and 8 WC) and 13 tests (2 CO, 5 WO and 6 WC) for the first and second position of trolley respectively were carried out.

During each test, as mentioned before, 5 Vectrinos disposed in 5 different vertical section of the ripple, acquired the velocity. Figure 4 shows the velocities acquired for three different case: CO, WO and WC. More precisely, the velocity along current direction ($U_x$) and along wave direction ($U_y$) are showed respectively in Figure 4a and 4b.

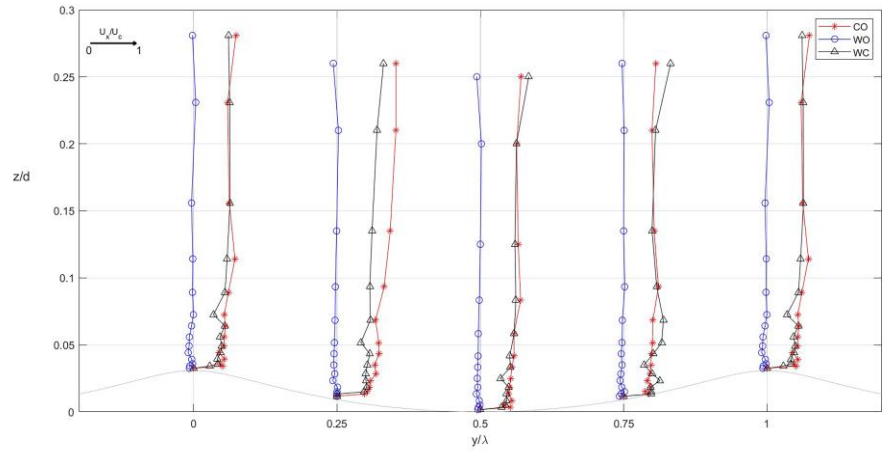


**(a)**

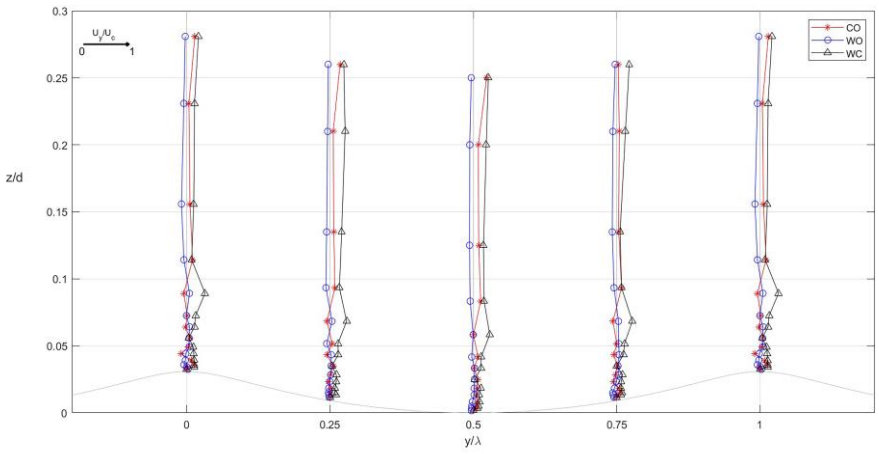


**(b)**

**Figure 4. Velocity profile along ripple in CO, WO an WC condition (*d*=0.6 m *T*=1 s and *H*=0.8 m). (a) velocity profile in current direction; (b) velocity profiles in wave direction.**

Figure 4a shows that, as expected, when the wave only velocity profile is averaged in time, all over the entire water column, the velocity is not sensibly different from zero or has slightly negative values.

However, at almost any measurement positions the contemporary presence of wave and current leads a deceleration of the flow in the outer layer with respect to the current only case.

In a previous study (Faraci et al. 2008) a similar analysis was carried out with the same wave conditions but sensibly smaller values of current conditions. In this latter case, the authors found an opposite behavior, i.e., an acceleration of the WC flow respect to the WO case. Probably this difference occurs because in the present study the current assumes much stronger values with respect to waves, thus revealing a key role to the ratio between current velocity to wave velocity, that will be further investigated in future studies.

When the time averaged velocity profiles in the wave direction are plotted, (Figure 4b) the current velocity is null under 0.1 *z/d*, whereupon it shows a slight deviation towards the beach that could be related to the presence of secondary steady current.

The wave only case, at 0.75 *z/d*, show an inversion of the velocity, i.e., a change of sign of the velocity vector, which seems to confirm the existence of recirculating cells in the lower part of the water column. Moreover, a small undertow current on the remaining *z/d* profile is present.

In WC case, it has been noticed that the acquired velocity profiles exhibit a similar behavior at all the measurement points. In particular, probably due to the presence of the above mentioned secondary steady current, above 0.5 *z/d* it veers in the direction of the beach.

The analysis of the flow field generating over the ripple profile is showed in Figure 5. This last was carried out by calculating the time average velocities in *y* and *z* directions.

A comparison between wave only (Figure 5a) and wave plus current (Figure 5b) case is showed in order to observed the variations that occur when the current superposed to the wave only. In the plots, the vectorial compositions, in the *y*-*z* plan, of the velocity along a ripple length are showed. The red arrow at the top right corner is a reference velocity and indicates also the wave propagation direction.

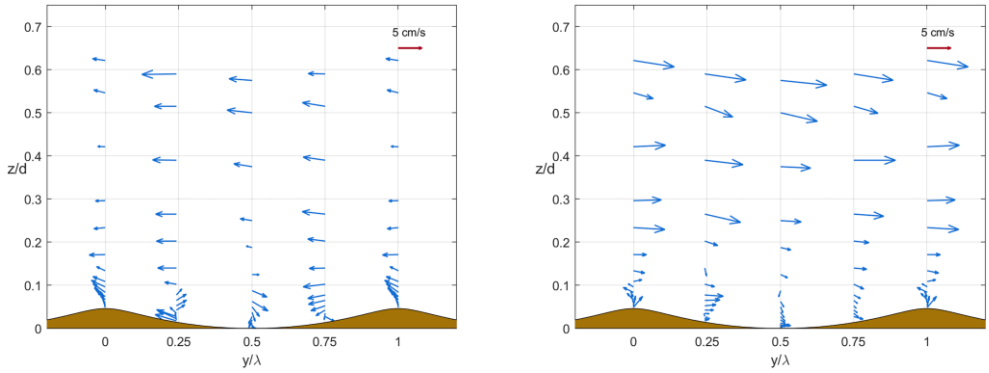


**Figure 5. Vectorial flow field along ripple. (*d*=0.4 m *T*=2 s and *H*=0.08 m). (a) WO case; (b) WC case.**

Near the bottom the formation of recirculating cells is clearly showed in both figures. In both cases they are formed below 0.15 *z/d* even if in the WC case the size of cells decreases. The size of the recirculating cells was estimated on the basis of the available vertical measurement transects, in particular, where the mean velocity reverses, there a recirculation cell can be found. The recirculating cell created in presence of current is more flatten than that of wave only case, indeed the height of recirculating cell extends until *z/d* =0.13 for WO case and *z/d*=0.1 for WC case.

From the position of the circulating cells (Figure 5a) that form near the bed, in the WO case the thickness of the boundary layer is identifiable up to about 0.15 *z/d* while in the WC case the thickness of the boundary layer is smaller and is about 0.1 *z/d.*

Moreover, Figure 5a shows, above 0.2 *z/d*, the presence of an undertow current that is equal to 1.74 cm/s. This value was calculated as the average velocity measured at the highest elevation by the 5 Vectrinos. It's possible to compare such value with a theorical undertow, calculated according to the method illustrated by Dean and Dalrymple (1991) validated for flat and smooth bed condition. The obtained result leads to a theorical undertow of 3.92 cm/s. The difference between the theoretical and the experimental value is probably due to the different bed roughness.

Observing the figure 5b the undertow cannot be identified being that the presence of the current, as one moves away from the bottom, compensates the velocity reversal effect.

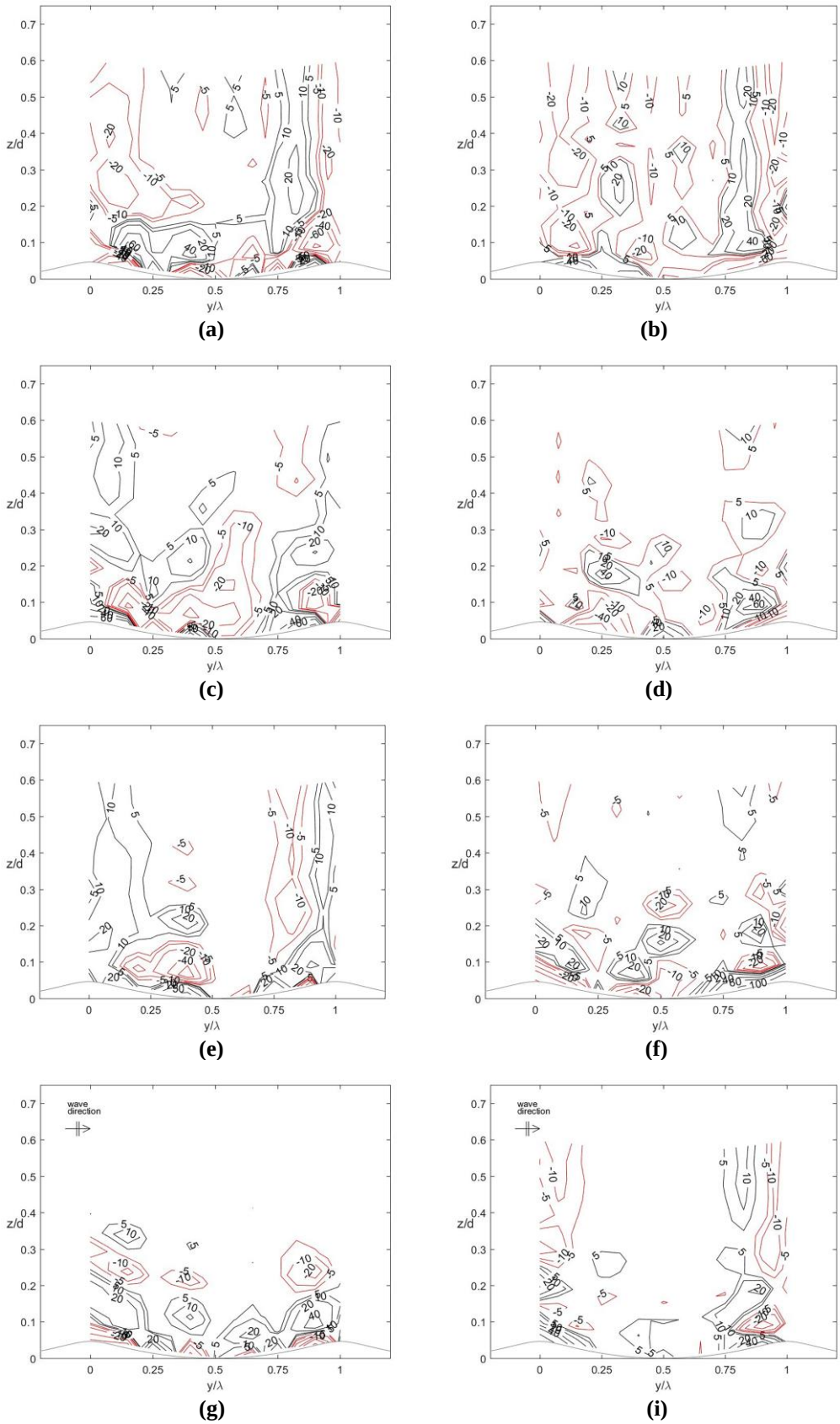


**Figure 6. Vorticity field for WO and WC case at four different phases during the wave period (*d*=0.4 m *T*=2 s and *H*=0.12 m). (a) WO case *π*/2 phase; (b) WC case *π*/2 phase; (c) WO case *π* phase; (d) WC case *π* phase; (e) WO case 3/2 *π* phase; (f) WC case 3/2 *π* phase; (g) WO case 2 *π* phase; (i) WC case 2 *π* phase.**

Finally, a vorticity study was performed on the experimental data to better understand the dynamics of sediment transport on a rippled bed in the presence of current or not.

In order to identify what are the effects that the superimposition of the current entails over a wave only case, in Figure 6 two tests with same water depth and same wave height and period, one for WO (left column) and the other for WC case (right column) are compared. To obtain a denser mesh of the acquired data, two identical flow condition tests at both configuration of trolley were identified. The measurements were properly overlapped and linearly interpolated so as to calculate the vorticity on a higher number of vertical sections along one ripple.

The eight figures show the contour plots of the vorticity made dimensionless by means of the wave period at four different phases during a wave cycle, starting with a phase of $\pi/2$ (wave crest) and with phase steps of $\pi/2$, respectively for wave only case (Figure 6 a-c-e-g) and wave plus current case (Figure 6 b-d-f-i).

The negative values, depicted in red, correspond to an anticlockwise vorticity, the positive values represented in black, to a clockwise vorticity. In the figures, the vorticity isolines present steps of 5.

At phase $\pi/2$, in WO case (Figure 6a) an anticlockwise vortex is created extending up to 0.2 *z/d* while in WC case (Figure 6b) this same appears flattens on the bed and reduced in intensity. The big clockwise vortex that remains attached near the bed and extends from crest to trough of the ripple, is divided into two smaller vortices in presence of current. The first one flattens on the bottom and the other one of minor intensity extend up to 0.3 *z/d*. From 0.2 *z/d* upwards in both conditions, WO and WC, the vorticity maintains the same trend even if, in the presence of current, its intensity slightly increases.

Observing now the Figures 6c and 6d, it's possible to observe that the presence of current reduces and pushes to the bottom the negative vorticity at the phase $\pi$. Indeed, both negative vortices which are clearly identified on the crests in the WO case, lower and extend close to the bottom in the presence of current. The positive vortex that is showed in WO case, flattens on the right ripple crest, raises and detaches from the ripple crest when the current superposes to the wave.

At the phase $3/2\ \pi$, the negative vorticity decreases in the WC case with respect to the WO case. Indeed, a negative vortex detaching from the left crest (Figure 6e) turns out reduced and flatten close to the bed in WC case (Figure 6f) while the two positive and negative vortices that in the WO case extend side by side, along the acquired water column, separate into smaller vortices up to 0.35 *z/d*. Moreover, in wave plus current condition the positive vorticity near the bed increase considerably at this phase.

Finally, the Figure 6g and Figure 6i show respectively the vorticity field at the phase $2\ \pi$ for wave only case and wave plus current case. At this phase in WO case the positive and negative vorticity is clearly identifiable along all the ripple below of 0.3 *z/d*, and out of this range is almost zero, while the superposition of the current on the wave alone, generates a fade of the vorticity at the ripple trough and an increase of vorticity along the entire water column.

It should also be noted that the symmetry between the two phases $\pi/2$ and $3/2\ \pi$ is clearly evident in both WO and WC conditions. Indeed, when the vorticity is negative at the phase $\pi/2$ the same trend but opposite in sign is identifiable at the phase $3/2\ \pi$, as shown in Figure 6a and 6e for wave only case and Figure 6b and 6f for wave plus current case.

Comparing the results of the present study with previous literature studies (Faraci et al. 2008 and Fredsøe et al. 1999), that however focused attention to the boundary layer only, it is possible to observe that, in the present case, the vortices that detach are not clearly identifiable at all phases.

Even in the previous studies, more or less at all phases, the vortices that detach from the ripple crest are identifiable. The clear identification is probably due to the shape of ripple crest. Indeed, flow separation occurs at the beginning of the half-cycle for sharp crests, earlier than it happens for round crests (Horikawa and Mizutani, 1992).

In Fredsøe et al. (1999) study, the ripple profile was characterized by a sharper crest than that used in this campaign. As well, in Fredsøe et al. experiments, the detachment of large vortices can be identified more easily and at almost all the stages, even though not always sharply. The detachment the vortices observed in Faraci et al. (2008) study, instead, is similar to present results since the profile of the ripples is the same in both campaigns.

## Conclusions

Investigation of orthogonal wave current interaction over rippled bed was the focus of this work. The data acquired during the experimental campaign in the framework of the WINGS project, were carried out in current only condition, wave only condition and wave plus current condition.

The analyses were showed an example of how flow and vorticity fields change when the current was superposed on the wave only and what are the variations when moving away from the bottom. The

presence of current led to flatten the recirculating cells that anyhow formed in both conditions. An undertow current was identified and calculated in wave only case, while in the wave plus current case this did not appear because the current compensated the effect of the velocity inversion.

Finally, the vorticity analysis showed that in both conditions WO and WC, a symmetry is noticed between the phases correspondent to crest and trough of wave cycle ($\pi/2$ e $3/2\pi$). The detachment of the vortices was identifiable, more or less, at all phase. Except for the wave trough, the presence of current induces an increase of vorticity outside the boundary layer and a decrease inside it.

Future works will be denoted to investigate more thoroughly the influence of the rippled bed on the flow and vorticity conditions when the wave and current parameters change.

## ACKNOWLEDGMENTS

The work described in this publication was supported by the European Community's Horizon 2020 Research and Innovation Programme through the grant to HYDRALAB-PLUS (TA WINGS-Waves plus currents Interacting at a right anGle over rough bedS), Contract no. 654110.

## REFERENCES

Dean, R.G.; Dalrymple, R.A. *Water Wave Mechanics for Engineers and Scientists*; World Scientific Publishing Company: Singapore, 1991; Volume 2.

Earnshaw, H.C.; Greated, C.A. Dynamics of ripple bed vortices. *Exp. Fluids* **1998**, *25*, 265–275.

Faraci, C.; Foti, E.; Musumeci, R.E. Waves plus currents crossing at a right angle: The rippled bed case. *J. Geophys. Res.* **2008**, *113*, 1–26.

Faraci, C.; Foti, E.; Marini, A.; Scandura, P. Waves plus currents crossing at a right angle: Sandpit case. *J. Waterw. Port Coast. Ocean Eng.* **2012**, *138*, 339–361.

Faraci, C.; Scandura, P.; Foti, E. Reflection of sea waves by combined caissons. *J. Waterw. Port Coast. Ocean Eng.* **2015**, *141*.

Faraci, C.; Scandura, P.; Musumeci, R.; Foti, E. Waves plus currents crossing at a right angle: Near-bed velocity statistics. *J. Hydraul. Res.* **2018**, *56*, 464–481.

Faraci, C.; Scandura, P.; Petrotta, C.; Foti, E. Wave-induced oscillatory flow over a sloping rippled bed *Water* **2019**, *11*, 1618.

Fredsøe, J.; Andersen, K.H.; Sumer, B.M. Wave plus current over a ripple-covered bed. *Coast. Eng.* **1999**, *38*, 177–221.

Goring, D.G.; Nikora, V.I. Despiking acoustic doppler velocimeter data. *J. Hydraul. Eng.* **2002**, *128*, 117–126.

Horikawa, H.; Mizutani, S. Oscillatory flow behaviour in the vicinity of ripple models. *Coast. Eng.* **1992**, *1993*, 2122–2135.

O'Donoghue, T.; Doucette, J.S.; Van Der Werf, J.J.; Ribberink, J.S. The dimensions of sand ripples in full-scale oscillatory flows. *Coast. Eng.* **2006**, *53*, 997–1012.

Petrotta, C.; Faraci, C.; Scandura, P.; Foti, E. Experimental investigation on sea ripple evolution over sloping beaches. *Ocean Dyn.* **2018**, *68*, 1221–1237.

Ranasoma, K.I.M.; Sleath, J.F.A. Combined oscillatory and steady flow over ripples. *J. Waterw. Port Coast. Ocean Eng.* **1994**, *120*, 331–346.

Ruggeri, A.; Musumeci, R.E.; Faraci, C. Wave-Current Flow and Vorticity Close to a Fixed Rippled Bed. *J. Mar. Sci. Eng.* **2020**, 8, 86

Scandura, P.; Vittori, G.; Blondeaux, P. Three-dimensional oscillatory flow over steep ripples. *J. Fluid Mech.* **2000**, *412*, 355–378.

Van der Zanden, J.; O'Donoghue, T.; Hurther, D.; Caceres, I.; McLelland, S.J.; Ribberink, J.S. Large-scale laboratory study of breaking wave hydrodynamics over a fixed bar. *J. Geophys. Res. Ocean.* **2017**, *122*, 3287–3310.

Yoon, H.-D.; Cox, D.T. Large-scale laboratory observations of wave breaking turbulence over an evolving beach. *J. Geophys. Res. Ocean.* **2010**, 115.C10.